emission spectral range agrees with the terahertz emission mechanism due to two-dimensional plasmons excited in the semiconductor matrix of the *n* type [39]. In this case, the observed increase in the intensity of terahertz emission with increasing the power of pumping can be related to an increase in the temperature of the electron gas, which facilitates thermal filling of plasmonic modes [40]. SEM studies with a subsequent Fourier transformation of images showed that the nanocomposites frequently exhibit a periodicity in the arrangement of nanocolumns, clusters, and pores. The fulfillment of the condition for the Bragg diffraction on structural inhomogeneities can favor an effective generation of terahertz emission. At the same time, the radiative decay of localized plasmons in sufficiently large In clusters has characteristic times corresponding to close frequencies that can indicate the involvement of these plasmons in the emission generation process.

We have considered effects related to the excitation of localized plasmons in metallic nanoparticles and their interaction with dipole transitions in a semiconductor. Experimental results are given for systems based on In(Ga)N. However, preliminary studies show that similar results can also be obtained for other semiconductors. This opens up great possibilities for the application of plasmonic effects in optoelectronics.

Acknowledgments. We are grateful to the researchers who took part in this work, in particular, to N A Gippius, V A Shalygin, V A Kosobukin, and T A Komisarova. This work was supported in part by the Russian Foundation for Basic Research (project Nos 07-02-00786a and 09-02-01305a) and by the Presidium of the Russian Academy of Sciences (program No. 27).

References

1. Ozbay E *Science* **311** 189 (2006)
2. Shalaev V M *Nature Photon.* **1** 41 (2007)
3. Wabuyele M B, Vo-Dinh T *Anal. Chem.* **77** 7810 (2005)
4. Bellessa J et al. *Phys. Rev. Lett.* **93** 036404 (2004)
5. Hetterich J et al. *IEEE J. Quantum Electron.* **43** 855 (2007)
6. Shen K-C et al. *Appl. Phys. Lett.* **93** 231111 (2008)
7. Kamaga C et al. *Appl. Phys. Lett.* **91** 173119 (2007)
8. Chen H-T et al. *Nature* **444** 597 (2006)
9. Christ A et al. *Phys. Rev. Lett.* **91** 183901 (2003)
10. Christ A et al. *Nano Lett.* **8** 2171 (2008)
11. Purcell E M *Phys. Rev. B* **69** 681 (1946)
12. Klimov V V *Usp. Fiz. Nauk* **178** 875 (2008) [*Phys. Usp.* **51** 839 (2008)]
13. Shubina T V et al. *Phys. Rev. Lett.* **92** 117407 (2004); **95** 209901 (2005)
14. Shubina T V et al. *Phys. Rev. Lett.* **93** 269702 (2004)
15. Shubina T V et al. *Phys. Status Solidi A* **202** 2633 (2005)
16. Shubina T V et al. *Phys. Status Solidi A* **203** 13 (2006)
17. Shubina T V et al. *J. Cryst. Growth* **288** 230 (2006)
18. Bartel T P et al. *Appl. Phys. Lett.* **91** 101908 (2007)
19. Shubina T V et al. *Phys. Status Solidi C* **4** 2445 (2007)
20. Crowell J, Ritchie R H *Phys. Rev.* **172** 436 (1968)
21. Kreibig U, Vollmer M *Optical Properties of Metal Clusters* (Berlin: Springer, 1995)
22. Moskovits M *Rev. Mod. Phys.* **57** 783 (1985)
23. Shubina T V et al. *Phys. Rev. B* **79** 153105 (2009)
24. Toropov A A et al. *Phys. Rev. Lett.* **103** 037403 (2009)
25. Jmerik V N et al. *J. Cryst. Growth* **301–302** 469 (2007)
26. Ivanov S V et al. *J. Cryst. Growth* **301–302** 465 (2007)
27. Lakowicz J R *Anal. Biochem.* **298** 1 (2001)
28. Farahani J N et al. *Phys. Rev. Lett.* **95** 017402 (2005)
29. Gersten J, Nitzan A *J. Chem. Phys.* **75** 1139 (1981)
30. Golovashkin A I et al. *Zh. Eksp. Teor. Fiz.* **51** 1623 (1966) [*Sov. Phys. JETP* **24** 1093 (1967)]
31. Westphalen M et al. *Solar Energy Mater. Solar Cells* **61** 97 (2000)
32. Shubina T V et al. *Phys. Status Solidi A* **202** 377 (2005)
33. Shubina T V et al. *Phys. Status Solidi C* **4** 2474 (2007)
34. Wu J et al. *J. Appl. Phys.* **94** 6477 (2003)
35. Komissarova T A et al. *Fiz. Tekh. Poluprov.* **43** 304 (2009) [*Semicond.* **43** 285 (2009)]
36. Shubina T V et al., in *Trudy 1-go Mezhdunar. Foruma po Nanotekhnologiyam, Moskva, 3–5 Dekabrya 2008* (Proc. 1st Int. Forum on Nanotechnologies) (Moscow: Rusnanotekh, 2008) p. 183
37. Shubina T V et al. *Izv. Ross. Akad. Nauk, Ser. Fiz.* **74** 68 (2010)
38. Shalygin V A et al. *Appl. Phys. Lett.* **90** 161128 (2007)
39. Mikhailov S A *SPIE Proc.* **3828** 139 (1999)
40. Höpfel R A, Vass E, Gornik E *Phys. Rev. Lett.* **49** 1667 (1982)

PACS numbers: 42.25.Fx, 78.20.Ls, **78.67.–n**
DOI: 10.3367/UFNe.0179.200909j.1012

Resonance scattering of light in nanostructured metallic and ferromagnetic films

V V Kurin

1. Introduction

In this report, we show that magnetooptical effects can be considerably enhanced in composite nanostructured metamaterials and ferromagnetic photonic crystals. The factors responsible for the enhancement can be both individual resonances in nanoparticles (plasma or geometrical) and collective resonances caused by multiple-scattering effects in lattices of nanoinhomogeneities.

Magnetooptical effects, which consist of a change in light polarization upon interaction with ferromagnetic materials, have been intensely studied for a sufficiently long time and are used in practice for the magnetooptical recording of information [1].

It seems obvious that magnetooptical effects can be substantially enhanced in nanostructured composite materials due to electrodynamic resonance effects, which have been given increased attention recently [2]. The nature of resonances can be different. In particular, these can be resonances connected with the excitation of natural modes of individual nanoinhomogeneities. An example of an enhancement of magnetooptical effects caused by individual resonances in a medium consisting of ferromagnetic nanospheres was first considered in Ref. [3].

Here, we demonstrate that an enhancement of magnetooptical effects can also be caused by resonance effects of another nature, such as the excitation of slowed-down waveguide modes, resonance scattering by nanowaveguides, and multiple scattering effects.

To demonstrate the effects of resonance enhancement of magnetooptical effects, we consider a simple model of an artificial medium consisting of a ferromagnetic film with cylindrical holes, assuming that the magnetization vector is directed along the normal to the film and the sizes of inhomogeneities are less than both the wavelength and the skin depth in the metal. Figure 1 shows a schematic of the scattering of an electromagnetic wave by such a structure and the basic excited waves.

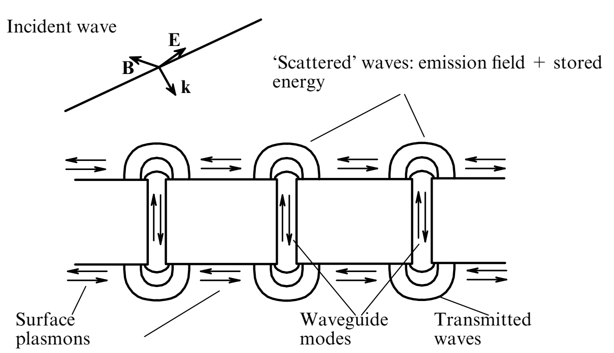

Figure 1. Scattering of an electromagnetic wave by a perforated ferromagnetic film (schematic). The main types of waves excited in the process of scattering are shown.

In the visible frequency range, the gyrotropy of a ferromagnet is connected with a gyroelectric mechanism [1] caused by the spin–orbital interaction [4], which manifests itself only in the off-diagonal elements of the dielectric constant tensor. The magnetic permeability can be set equal to the unit diagonal tensor $\mu_{ik} = \delta_{ik}$. In the coordinate system where the z axis is oriented along the magnetization vector $\mathbf{M}$ and the vector $\mathbf{r}_\perp = (x, y)$ lies in the perpendicular plane, the dielectric constant tensor of the ferromagnetic film is analogous in structure to the tensor of the electron gas in a magnetic field and is written in the form

$$\hat{\varepsilon} = \begin{pmatrix} \varepsilon & \mathrm{i}g & 0 \\ -\mathrm{i}g & \varepsilon & 0 \\ 0 & 0 & \eta \end{pmatrix}, \qquad (1)$$

where ε and η are respectively the longitudinal and transverse dielectric constants and g is the gyrotropy parameter proportional to the magnitude of the magnetization. A characteristic magnitude of gyrotropy of a typical ferromagnet Co is $g \sim 10^{-2}$, which corresponds to the effective magnetic field 10^6 G. The diagonal elements of the tensor $\varepsilon \approx \eta \sim 1$ have an order of magnitude characteristic of metals.

2. Propagation of waves in a ferromagnetic nanowaveguide

It is natural to begin solving the problem of scattering by a perforated film by studying eigenmodes of a cylindrical nanohole. We assume that the magnetization vector is parallel to the waveguide axis, which is directed along the normal to the film. We note that such a direction of magnetization in a continuous film is sufficiently difficult to realize in view of the large contribution of the magnetostatic energy; therefore, to achieve the vertical magnetization, ferromagnets with a large internal anisotropy must be used. It is known, for example, that such a direction of $\mathbf{M}$ can be realized in films of CoPt and CoPd [5, 6]. But we note that the magnetic state of the film can change because of the presence of openings in the film, because the fields in the openings make a contribution to the free energy of the magnet, and the magnetic state of a film with nanoinhomogeneities must be determined with the aid of micromagnetic calculations.

We consider the problem of eigenwaves of a nanowaveguide in a ferromagnet with the magnetization along the waveguide axis. By finding solutions of the Maxwell equations in the form $(\mathbf{E}, \mathbf{B}) \sim (\mathbf{e}, \mathbf{b}) \times \exp(\mathrm{i}\omega t + \mathrm{i}m\varphi + \mathrm{i}hz)$, where ω is the frequency, m is the azimuthal index, and h is the longitudinal wave number, and by matching the solutions for the external and internal regions according to the requirement of the continuity of the tangential (z, φ) component of the fields, we obtain a dispersion relation, which in the case of weak gyrotropy takes the form

$$\begin{aligned} \left[\varepsilon_{\mathrm{i}} f(x) - \eta F(y)\right]\left[f(x) - F(y)\right] - \frac{m^2\zeta^2}{u^2}\left(\frac{1}{x^2} + \frac{1}{y^2}\right)^2 \\ = \frac{gm}{y^4 x^2}\left[(2\zeta^2 + x^2)\big(x^2 f(x) + y^2 F(y)\big) \right. \\ \left. + \zeta^2(x^2 + y^2)\frac{\partial y^2 F(y)}{y\,\partial y}\right]. \qquad (2) \end{aligned}$$

Here, we let ε_{i} denote the dielectric constant inside the waveguide and introduce dimensionless transverse wave numbers $x = q_{\mathrm{i}} a$ and $y = \mathrm{i}q_{\mathrm{e}} a$ (where q_{i} and q_{e} are the transverse wave numbers for the internal and external regions), dimensionless longitudinal wave number $\zeta = ha$ and frequency $u = ka$, a dimensionless plasma frequency $v = \omega_{\mathrm{p}} a/c$, and $\eta = 1 - v^2/u^2$, where a is the nanowaveguide radius and $k = \omega/c$ is the wave number in the vacuum; $f(x) = J_m'(x)/\big(xJ_m(x)\big)$ and $F(y) = -K_m'(y)/\big(yK_m(y)\big)$, where J_m and K_m are the respective Bessel and MacDonald functions.

The vanishing of the left-hand side of Eqn (2) yields a well-known dispersion relation for a waveguide in an isotropic nonferromagnetic metal; the right-hand side expresses first-order corrections in g due to gyrotropy, which lift the degeneracy in the azimuthal index m. An incident plane wave can excite only waves with $m = \pm 1$; we analyze these waves in the case of narrow channels, where $x,\ y \ll 1$. Expressing the frequency $x,\ y \ll 1$, the longitudinal wave number u, and the permeability ζ in terms of the transverse wave numbers and using the undisturbed dispersion relations $\zeta^2(\varepsilon_{\mathrm{i}} - 1)^{-1}(\varepsilon_{\mathrm{i}} x^2 + y^2 - \varepsilon_{\mathrm{i}} v^2)$, $u^2 = (\varepsilon_{\mathrm{i}} - 1)^{-1}(x^2 + y^2 - v^2)$, we obtain a closed equation for x and y, which is solved explicitly using the expansions $f = x^{-2} - 0.25$ and $F = y^{-2} + \ln 2(\gamma y)^{-1}$ that are valid in the limit of a narrow waveguide and a small gyrotropy parameter g. The characteristic dispersion curves are shown in Fig. 2.

As $h \to 0$, the frequencies of modes with the azimuthal indices $m = \pm 1$ tend to the frequency of the surface plasmon $\omega_{\mathrm{sp}} = \omega_{\mathrm{p}}(1 + \varepsilon_{\mathrm{i}})^{-1/2}$, irrespective of the size of the holes. This corresponds to the well-known fact that even an arbitrarily narrow waveguide in a real metal can carry a dipole mode.

We now consider a change in the polarization with the propagation of a wave in the waveguide. For this, we assume

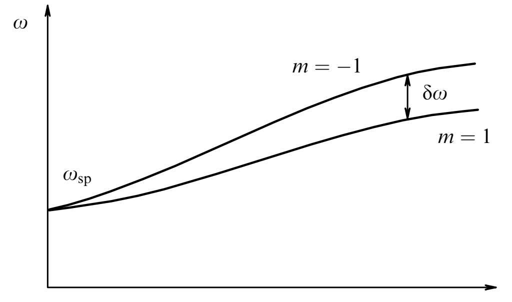

Figure 2. Dispersion curves of dipole waveguide modes in a ferromagnetic nanowaveguide.

that the direction of polarization of the waveguide mode is the direction of the electric field vector at the waveguide axis. In the case of a small gyrotropy parameter g, we can use the correct zero-approximation eigenvectors and find that the polarization rotation angle, which is given by

$$\theta = \big(h_1(\omega) - h_{-1}(\omega)\big)\, d \approx \frac{\delta\omega\, d}{v_{\mathrm{g}}}\,,$$

is anomalously large as a result of a strong slowdown of waves in the nanowaveguide. Here, $h_{\pm 1}$ are the longitudinal wave numbers of waves with the azimuthal indices $m = \pm 1$, d is the thickness of the ferromagnetic film, $\delta\omega$ is the splitting of dispersion curves with $m = \pm 1$, and v_{g} is the group velocity. We note that the wave slowdown increases not only the rate of Faraday rotation but also the damping of the waveguide modes. The characteristic attenuation length of the waveguide modes depends on the diameter of the waveguide, and is approximately 10 μm for the diameter of the order of 50 nm.

3. Individual resonance in the case of scattering by a single waveguide

In this section, we consider the problem of the transmission and reflection of external electromagnetic radiation upon interaction with a single nanowaveguide in a ferromagnetic film. As previously, we assume that the magnetization is perpendicular to the surface of the film. To solve the problem, we must estimate the efficiency of the excitation of waveguide modes by a wave incident on the upper boundary and the excitation of the transmitted and reflected waves by the arising waveguide modes. The problem can be solved approximately as follows. It is well known [7, 8] that a hole in the metal can be replaced by effective electric and magnetic currents concentrated on both sides of the film in a region with the thickness of the order of the skin depth in the metal, as is shown in Fig. 3.

Near the ends of the waveguide, we separate regions with the depth and the radius of the order of the skin depth in the surrounding metal, in which the effective magnetic and electric currents flow [4], and assume that their multipole moments are known; hence, we find the external fields with respect to these regions. In the free space before the film, this is a set of the fields of multipoles, incident wave, and the wave reflected from the flat surface; in the waveguide, these are only the fields of the counterpropagating waves; in the space on the other side of the film, these are only the fields of the multipoles. We must also write a solution for the internal regions of the ends of the waveguide. The next step consists in matching the tangential components of the internal and external representations of the fields on the surface that separates these regions, and finding the amplitudes of an infinite number of modes in the waveguide, including the nonpropagating ones, as well as of the magnitudes of all multipole moments and the distribution of the field in the vicinities of the waveguide ends.

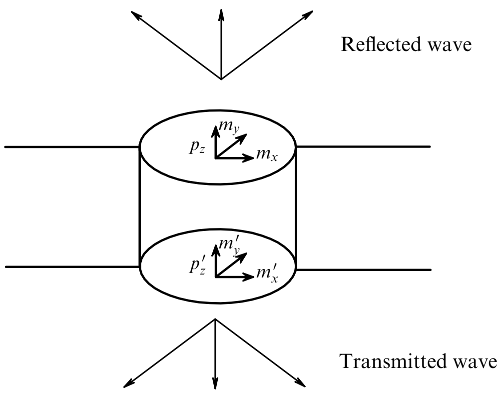

Figure 3. Response of a nanowaveguide to external radiation. Effective dipole moments.

If such a procedure were carried out, we would obtain an exact solution of the problem. Unfortunately, this solution leads to complex integral equations, which can be solved only numerically. However, for nanowaveguides with a diameter that is small compared with the wavelength and the skin depth, we can obtain an approximate solution by restricting ourselves to only fields of dipoles outside the nanowaveguide and to only propagating waves inside it. For simplicity, we neglect the intermediate region and match the components of the solution $\mathbf{E}_\perp$ and $\mathbf{B}_\perp$ at one point, e.g., the point on the z axis located at a distance equal to the waveguide radius from the film plane. In this approach, we ignore effects connected with the existence of plasma resonance at the frequency of the surface plasmon ω_{sp}, assuming that the wave frequency is far from it.

We consider the case of normal incidence, where the scattering occurs only in the magnetodipole channel and the magnetic dipoles have only components that are perpendicular to the z axis. We assume that the incident wave is linearly polarized along the x axis. We decompose the $(\mathbf{E}, \mathbf{B})_\perp$ fields on the z axis and the magnetic dipole moments on one side and the other side of the film $\mathbf{M}^{\mathrm{L}}$ and $\mathbf{M}^{\mathrm{R}}$ into the left-handed and right-handed components $(E, B, M)_\pm = (E, B, M)_x \pm \mathrm{i}(E, B, M)_y$, which are eigenvectors for the field both outside and inside the waveguide; for the field on the side of the wave incidence (L), we then write these components as

$$E_\pm = \exp(\mathrm{i}kz) - \exp(-\mathrm{i}kz) \pm kM^{\mathrm{L}}_\pm (\mathrm{i}k - |z|^{-1})\,\frac{\exp(\mathrm{i}k|z|)}{|z|}\,,$$

$$B_\pm = \pm\mathrm{i}\big[\exp(\mathrm{i}kz) + \exp(-\mathrm{i}kz)\big] + M^{\mathrm{L}}_\pm (k^2 + \mathrm{i}k|z|^{-1} - z^{-2})\,\frac{\exp(\mathrm{i}k|z|)}{|z|}\,;$$

next, for the field on the waveguide axis,

$$E_\pm = c_\pm \exp(\mathrm{i}k_\pm z) + d_\pm \exp(-\mathrm{i}k_\pm z)\,,$$

$$B_\pm = \pm\mathrm{i}\,\frac{k_\pm}{k}\,\big[c_\pm \exp(\mathrm{i}k_\pm z) + d_\pm \exp(-\mathrm{i}k_\pm z)\big]\,,$$

where $k_\pm$ is the solution of dispersion equation (2), and for the transmitted field (R),

$$E_\pm = \mp kM^{\mathrm{R}}_\pm \big(\mathrm{i}k - |z|^{-1}\big)\,\frac{\exp(\mathrm{i}k|z|)}{|z|}\,,$$

$$B_\pm = M^{\mathrm{R}}_\pm \big(k^2 + \mathrm{i}k|z|^{-1} - z^{-2}\big)\,\frac{\exp(\mathrm{i}k|z|)}{|z|}\,.$$

In the last two expressions, the coordinate z is referenced to the right end of the waveguide. In all the expressions, we omit the common factor $\exp(-\mathrm{i}\omega t + \mathrm{i}m\varphi)$, and in the expression for the reflected wave, we neglect the difference from -1 for the reflection coefficient from the metal and ignore the change in the polarization. These simple effects can be easily taken into account, if necessary, in the framework of the suggested scheme. Furthermore, in calculating fields of the dipoles, we disregarded the excitation of a surface plasmon. By matching the solutions, we obtain the magnitudes of the magnetic dipole moments on the left-hand and right-hand boundaries of the nanowaveguide and the amplitudes of the modes propagating in the waveguide. The expression for the magnetic moments on the left-hand boundary of the layer is written as

$$M_{\pm}^{\mathrm{L}} = \mp \mathrm{i}\,\frac{(h_{\pm}/k)\,G^{E} - \mathrm{i}G^{H}\tan(h_{\pm}d)}{(h_{\pm}/k)\,G^{E}G^{H} - (\mathrm{i}/2)\left[(G^{H})^{2} + (h_{\pm}^{2}/k^{2})(G^{E})^{2}\right]\tan(h_{\pm}d)}\,,$$

and that on the right-hand boundary, as

$$M_{\pm}^{\mathrm{R}} = \pm \mathrm{i}\,\frac{(h_{\pm}/k)\,G^{E}\cos^{-1}(h_{\pm}d)}{(h_{\pm}/k)\,G^{E}G^{H} - (\mathrm{i}/2)\left[(G^{H})^{2} + (h_{\pm}^{2}/k^{2})(G^{E})^{2}\right]\tan(h_{\pm}d)}\,,$$

where d is the film thickness, k is the wave number in the vacuum, and G^E and G^H are the electric and magnetic components of the magnetodipole Green's function, which are defined as $G^E = -\mathrm{i}ka^{-2}(\mathrm{i}ka - 1)\exp(\mathrm{i}ka)$ and $G^H = G^E - a^{-3}\exp(\mathrm{i}ka)$. These expressions resemble the formulas for the coefficients of reflection of a plane wave from a layer of a dielectric medium and of the transmission through this medium; but we note that, unlike the law of conservation of the energy flux in the case of a layer, the energy flux conservation law in the case under consideration is given by the so-called optical theorem:

$$\mp \mathrm{Re}\, M_{\pm}^{\mathrm{L}} = \frac{1}{3}\,k^{3}\left(|M_{\pm}^{\mathrm{L}}|^{2} + |M_{\pm}^{\mathrm{R}}|^{2} + Q\right),$$

where Q denotes the losses in the waveguide. The left-hand side of this expression represents the flux lost from the incident and reflected plane waves. The formulas for $M_{\pm}^{\mathrm{L,R}}$ define it as a positive definite quantity. However, the condition that this flux is equal to the sum of dissipated and absorbed fluxes is violated in general because the matching conditions are here satisfied only approximately. Therefore, the expressions obtained are applicable only under the condition of the smallness of radiation losses compared to the dissipation. Given the formulas for $M_{\pm}^{\mathrm{L,R}}$, we can easily find the Cartesian coordinates of the dipole moments M_x and M_y.

Figure 4 qualitatively displays the frequency dependence of the polarization parameters for the backward scattering of linearly polarized radiation in the near-resonance region $kd \sim \pi$. The figure shows the dependence of the angle of the inclination of the major axis of the ellipse of polarization of the magnetic dipole moment with respect to the magnetic field direction in the incident wave of polarization ($\tan\theta = \mathrm{Re}(M_x^{\mathrm{L}}/M_y^{\mathrm{L}})$; dashed curve), and the dependence of the ratio of the minor semiaxis of the ellipse of polarization to the major semiaxis, $b \approx \mathrm{Im}(M_x^{\mathrm{L}}/M_y^{\mathrm{L}})$ (solid curve), on the dimensionless frequency $\Omega = u/u_{\mathrm{res}}$ in the vicinity of one of the resonances, whose frequencies are determined by the relations $h_{+1}(u)\,d \approx h_{-1}(u)\,d \approx n\pi d$. Analogous resonance effects are also to be observed in the case of radiation passing through the film. It is seen from the figure that the angle of the inclination of polarization increases substantially as the resonance is approached. For typical film parameters and room temperature, an approximately tenfold resonant enhancement of the magnetooptical effect can be expected in comparison with that in a continuous ferromagnetic film. For cooled samples, the resonances must be even more clearly pronounced. It is interesting to note that the resonance magnetooptical effect under consideration is characterized by a change in the sign of the rotation angle of the polarization plane in the near-resonance region.

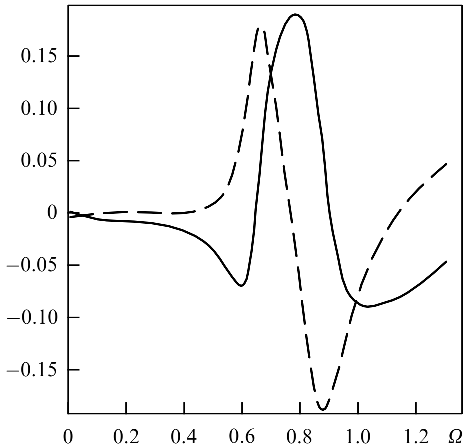

Figure 4. Typical frequency dependence of the parameters of the ellipse of polarization of reflected light in the vicinity of one of the resonances with a mode of a finite waveguide. The solid curve shows the ratio of the major axes of the ellipse of polarization of the magnetic dipole moment; the dashed curve demonstrates the behavior of the angle of rotation of its major axis with respect to the polarization direction in the incident wave.

4. Multiple scattering effects

If we now consider a lattice of waveguides instead of one nanowaveguide, then the external electromagnetic field in the vicinity of the waveguide ends is determined not only by the fields of waves incident on the metal surface and reflected from it but also by the fields created by effective sources located at the ends of other nanowaveguides.

In the case of a regular lattice, the interaction of individual nanoinhomogeneities is resonantly enhanced when some diffraction maximum becomes grazing, and the diffracted field undergoes a transformation from the field of radiation to the field 'pressed' to the surface. Resonances of this type were discovered experimentally in [9] and were described theoretically in [10]. The experimentally measured resonant enhancement of the local field considerably exceeds the enhancement of the field on single particles, and reach values of the order of several thousand for gold nanoparticles. It is absolutely obvious that these collective resonances, which can naturally be called diffraction resonances, also strongly influence the magnetooptical effects.

The resonance scattering must be described with due care because seemingly natural approximations, which lead to the replacement of an infinite system for the amplitudes of natural waves by a finite system as in Section 3, or, for example, the approximations of a given polarizability described in [8], lead to a violation of the physically natural conservation laws. This restricts the field of the applicability of the formulas obtained to the condition of the domination of collisional losses over radiative losses. It is obvious that with an increase in the size of the system, the role of collisional losses in the case of diffraction resonance decreases because of an increase in the stored energy, and the requirements concerning the accuracy of the calculations of radiation effects should increase considerably. To achieve physically reasonable results, it is usually necessary to use numerical methods [10]. However, we here describe an example of a problem that allows a self-consistent analytic solution; we also show how it can be extended to the case of a gyrotropic medium.

We consider the simple problem of scattering of a plane electromagnetic wave by a lattice of equispaced (at points $x = 0, y = jL$) narrow parallel cylinders with the generatrices parallel to the z axis. Let the plane of incidence be perpendicular to the generatrices of the cylinders and let the angle of incidence be χ. In this case, the problem splits into two scalar problems, which correspond to two independent polarizations, H and E, with the magnetic and electric field vectors directed along the z axis. We perform calculations for the H polarization, which is more interesting because with this polarization, upon scattering by a cylinder, there exists an individual quasistatic resonance whose frequency is determined from the equation $\varepsilon + 1 = 0$. The calculations for the second polarization are conducted analogously. We write the expressions for the fields outside and inside the cylinders as:

$$B_z^{\text{out}} = \exp(\mathrm{i}k_x x + \mathrm{i}k_y y) + \sum_{m,j} \mathrm{i}^m \exp(\mathrm{i}m\varphi_j)\, D_m^j H_m^1(k\rho_j)\,,$$

$$B^{\text{in}} = \sum_{m,j} \mathrm{i}^m \exp(\mathrm{i}m\varphi_j)\, F_m^j J_m(k\sqrt{\varepsilon}\rho_j)\,, \tag{3}$$

where D_m^j and F_m^j are the multipole coefficients, which respectively characterize the outside and inside fields, $H_m^1(k\rho_j)$ is the Hankel function of the first order, which describes the diverging wave, $J_m(k\rho_j)$ is the Bessel function, and the radius ρ_j is referenced to the center of the jth cylinder. Using an expansion of the plane wave in Bessel functions and Graf's addition theorem for the cylinder functions of the shifted argument $\boldsymbol{\rho}_j = \mathbf{x}_0 x + \mathbf{y}_0(y - jL)$, where L is the distance between the cylinders, we represent the external field in the vicinity of the jth cylinder as

$$B_z = \sum_m \mathrm{i}^m \exp(\mathrm{i}m\varphi)\Big\{J_m(k\rho_j)\big[\exp(\mathrm{i}kLj\sin\chi - \mathrm{i}m\chi)$$
$$+ \sum_{n,\,l<j} D_{-n}^l H_{n+m}^1(kL|j-l|)$$
$$+ \sum_{n,\,l>j} (-1)^{m+n} D_{-n}^l H_{n+m}^1(kL|j-l|)\big] + D_m^j H_m^1(k\rho_j)\Big\}. \tag{4}$$

Thence, it follows that as a result of the emission from cylinders with numbers $l \neq j$, a renormalization of the incident wave occurs. If we now match the external and internal tangential fields B_z and $E_\varphi = \mathrm{i}/(\varepsilon k)\,\partial B_z/\partial\rho$ on the surface of this cylinder, we obtain a set of equations for the multipole coefficients D_m^j and F_m^j. In contrast to the procedure used in Section 3, this approach the boundary conditions to be satisfied exactly over the entire surface of the cylinder. This method of solving the problem is an application of the well-known Korringa–Kohn–Rostoker method [11, 12], which was first proposed for scalar quantum mechanical problems and is widely used in calculations of the band structure of solids. (For the extension of this method to vector electrodynamic problems, see [13].) In Ref. [14], an analogous method was used to numerically solve the problem of scattering of an electromagnetic wave by a lattice of isotropic cylinders.

Now, using the translational symmetry of the problem, we perform a discrete Fourier transformation with respect to the order number of cylinders j. The formulas for the direct and inverse transformations are determined by the relation

$$D_m^j = \int_{-\pi/L}^{\pi/L} D_m(q)\exp(\mathrm{i}qLj)\,\frac{L\,\mathrm{d}q}{2\pi}\,,$$

$$D_m(q) = \sum_j D_m^j \exp(-\mathrm{i}qLj)\,. \tag{5}$$

The transformation for the incident wave has the form $\delta(qL - kL\sin\chi)\exp(-\mathrm{i}m\chi)$; therefore, by isolating this singularity, $(D_m(q), F_m(q)) = \delta(qL - kL\sin\chi)(D_m, F_m)$, we obtain the following set of equations for the coefficients (D_m, F_m):

$$J_m(ka)\Big[\exp(-\mathrm{i}m\chi) + \sum_n D_{-n}G_{n+m}(kL, \sin\chi)\Big]$$
$$+ D_m H_m^1(ka) = F_m J_m(k\sqrt{\varepsilon}a)\,,$$
$$J_m'(ka)\Big[\exp(-\mathrm{i}m\chi) + \sum_n D_{-n}G_{n+m}(kL, \sin\chi)\Big]$$
$$+ D_m' H_m^1(ka) = \frac{1}{\sqrt{\varepsilon}}\,F_m J_m'(k\sqrt{\varepsilon}a)\,, \tag{6}$$

which is identical in structure to the set that determines the multipole coefficients in the case of wave scattering by a single cylinder. The only difference is in the additional term in brackets, which describes the renormalization of the incident wave. The coefficients G_m that are responsible for the renormalization are given by

$$G_m(kL, \sin\chi) = \sum_{j>0} H_m^1\big(kL|j|\big)$$
$$\times\big[\exp(\mathrm{i}kLj\sin\chi) + (-1)^m\exp(-\mathrm{i}kLj\sin\chi)\big]\,.$$

If we now assume that the radius of the scatterers is small in comparison with the length of the optical wave, such that $ka \ll 1$, then the main contributions come from the dipole components $D_{\pm1}$ and the set of equations (6) transforms into a set of four equations for four unknowns $D_{\pm1}$ and $F_{\pm1}$. The two renormalization factors G_0 and G_2 enter this set as coefficients.

Introducing the coefficients $2(D,F)_y = (D,F)_1 + (D,F)_{-1}$ and $2\mathrm{i}(D,F)_x = (D,F)_1 - (D,F)_{-1}$, we see that the equations for them split and can easily be solved. We here write only expressions for the dipole moments that determine the diffracted field:

$$D_{x,y} = \begin{pmatrix} \sin\chi \\ -\cos\chi \end{pmatrix}$$
$$\times \frac{J_1'(u)\,J_1(\sqrt{\varepsilon}u) - (1/\sqrt{\varepsilon})\,J_1(u)\,J_1'(\sqrt{\varepsilon}u)}{\big[H_1^1(u) + G_{x,y}J_1(u)\big]\,J_1(\sqrt{\varepsilon}u) - (1/\sqrt{\varepsilon})\big[H_1^1(u) + G_{x,y}J_1(u)\big]\,J_1'(\sqrt{\varepsilon}u)}\,, \tag{7}$$

where $u = ka$ and where the Cartesian renormalization factors are linear combinations of G_m,

$$G_x = \sum_{j=1}^{\infty} \left[H_0^1(jkL) - H_2^1(jkL)\right] \cos(kLj\sin\chi)\,,$$

$$G_y = \sum_{j=1}^{\infty} \left[H_0^1(jkL) + H_2^1(jkL)\right] \cos(kLj\sin\chi)\,. \tag{8}$$

For small $u \ll 1$, the cylinder functions can be expanded into a series, with the result

$$D_{x,y} = \frac{\pi u^2}{4\mathrm{i}} \left\{ \frac{\varepsilon+1}{\varepsilon-1} - \frac{\pi}{4}\,\mathrm{i}u^2(1 + \mathrm{Re}\,G_{x,y}) - \frac{u^2}{8}\left(\left[\varepsilon + 2 - 4\left(\ln\frac{u}{2} + \gamma\right)\right] - 2\pi u^2\,\mathrm{Im}\,G_{x,y}\right)\right\}^{-1}, \tag{9}$$

which allows a simple physical interpretation. We isolated three groups of terms in the denominator. The first is responsible for the individual quasistatic polarization; the remaining two groups give wave corrections. The imaginary part of the denominator describes the energy losses, including those for emission. The real part gives reactive corrections and determines the resonance frequency. In the case of a real dielectric constant ε, the only channel of losses is radiative losses, which are determined by the second term in the denominator. The collective effects of the renormalization of the fields of emission and 'pressed-to-surface' nonradiative fields are determined by the factors $G_{x,y} = G_0 \mp G_2$, the typical dependences of the real and imaginary parts for which are shown in Fig. 5. Both the real and imaginary parts of the factors $G_{0.2}$ have square-root singularities in the vicinity of the frequencies or incidence angles at which some diffraction maxima become grazing and the field propagating along the z axis is converted into a nonpropagating one, 'pressed' to the lattice of cylinders. It is natural that for finite lattices or for lattices with a disorder, neither an infinite increase nor an infinitely sharp discontinuity occurs. The asymptotic behavior near the diffraction peak, which can be found analytically (for example, see [15], Eqns 8.522), is determined by the real and imaginary parts of the expression

$$G_{0.2} \sim \left[(kL)^2 - (2\pi l \pm kL\sin\chi)^2\right]^{-1/2}, \tag{10}$$

where l is an integer that corresponds to the order number of the diffraction peak. From the graphs presented in Fig. 5, it can be seen that the behavior of the real and imaginary parts is described by characteristic resonance curves of an asymmetric shape, which is specularly symmetric relative to the singularity point. We note that the factor G_y does not become infinite, apparently because the y components of the dipole moments interact with each other via quasistatic fields, since the dipoles do not emit radiation along themselves.

Now, using the known coefficients (7) and inverting the discrete Fourier transformation, we can find the local multipole coefficients $(D,F)_m^j = (D,F)_m \exp(\mathrm{i}kLj\sin\chi)$ and calculate the scattered field and the fields inside the cylinders. An analysis of the far field with known coefficients is carried out in the standard manner [10], by passing from expansion (3) to an expansion in terms of spatial harmonics of the form

$$B_z^{\mathrm{scatter}} = \sum_l C_l \exp\left[\mathrm{i}\sqrt{k^2 - \left(k\sin\chi + \frac{2\pi l}{L}\right)^2}\,x + \mathrm{i}\left(k\sin\chi + \frac{2\pi l}{L}\right)y\right]. \tag{11}$$

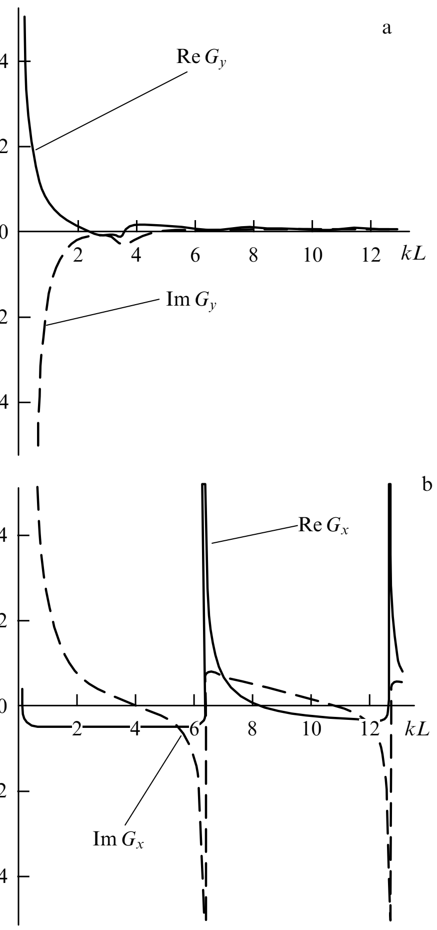

Figure 5. Typical frequency dependences of the real (solid curves) and imaginary (dashed curves) parts of the factors of the renormalization of the Cartesian components of the dipole moments (a) G_y and (b) G_x, which determine the dissipative and reactive contributions of the collective field. The graphs are plotted at a fixed angle of incidence χ, $\sin\chi = 0.8$.

An analysis of the behavior of the coefficients C_i shows that near the edge of an lth diffraction maximum, the power radiated into an appropriate partial wave $P_l \sim \mathrm{Re}\left[k^2 - (k\sin\chi + 2\pi l/L)^2\right]^{1/2}|C_l|^2$ as a function of frequency has a threshold nature. The power radiated into an open channel as a function of frequency has a discontinuity in the derivative. The situation here is in many respects analogous to that characteristic of the behavior of reaction cross sections near reaction thresholds [16].

We now discuss the consequences that can result from the nonperpendicularity of the plane of incidence to the axis of the cylinders and from the presence of gyrotropy caused by the ferromagnetism of the dielectric cylinders. Let the ferromagnet magnetization vector, as previously, be directed along the axes of the cylinders. We first note that the existence of a wave vector of the incident wave parallel to the cylinder axis in the absence of gyrotropy leads to a hybridization of the E and H modes, which until now were accepted to be independent. If we supply the coefficients D and F with an additional index taking values E or H depending on which of the z component is different from zero, and write equations analogous to (6), these equations are no longer be diagonal with respect to this additional index. But the degeneracy in the azimuthal number $m = \pm 1$ is preserved. Then, by introducing Cartesian components, we can reduce the set of the eighth order for $(D, F)^{\mathrm{E,H}}_{\pm 1}$ to two sets of the fourth order. In this case, as a result of the hybridization of electric and magnetic components, there appear individual resonances determined by the vanishing the factor $\varepsilon + 1$ in the electric components. The renormalization factors G, which are responsible for the collective effects, also change; however, because of the retention of the polarization degeneracy, the new $G_y^{\mathrm{E,H}}$ components are then determined by only quasistatic fields, as before.

If we take the gyrotropy into account, then in the dipole approximation, the system analogous to (6) remains a general system of the eighth order, and hybridization must also occur in the vector x and y components of the electric and magnetic dipole moments, causing a mixing of the equations for the x and y projections of the fields and dipole moments. In the dipole components $D_{\pm 1}$, all the resonances are then present, both individual and collective. Because these resonances are shifted in the different components due to the gyrotropy, resonance effects of the polarization plane rotation must be observed in both the reflected and the transmitted radiation. Especially promising for the enhancement of the magnetooptical effects seems to be the diffraction resonance; because of the presence of singularities in frequency in the derivatives of the excitation coefficient of the open channel, the difference in the excitation coefficients of the left-handed and right-handed components are anomalously large, which should lead to anomalously strong Kerr and Faraday effects. It is well possible that a significant enhancement of magnetooptical effects observed recently in experiments [17] is connected precisely with this mechanism.

5. Conclusions

We have considered the influence of nanoinhomogeneities on the magnetooptical effects in ferromagnetic films. It has been demonstrated that as a result of the retardation of waves in nanowaveguides and the presence of individual internal resonances in the waveguides and collective effects of multiple scattering, the magnetooptical effects can be considerably enhanced. We expect that the effects of a resonant enhancement of magnetooptical effects can be used for creating new devices for the recording and processing of information and for the diagnostics of magnetic states in composite ferromagnetic films.

Acknowledgments. I am very grateful to A A Zharov and A A Andronov for numerous and fruitful discussions. This work was supported in part by the Russian Foundation for Basic Research (project Nos 08-02-00379 and 09-02-00863), Program No. 27 of the Presidium of the Russian Academy of Sciences, and Program No. II.5 of the Division of Physical Sciences, Russian Academy of Sciences.

References

1. Mishin D D *Magnitnye Materialy* (Magnetic Materials) (Moscow: Vysshaya Shkola, 1991)
2. Genet C, Ebbesen T W *Nature* **445** 39 (2007)
3. Zharov A A, Kurin V V *J. Appl. Phys.* **102** 123514 (2007)
4. White R M *Quantum Theory of Magnetism* 2nd ed. (Berlin: Springer-Verlag, 1983) [Translated into Russian (Moscow: Mir, 1985) p. 197]
5. Mukai R, Uzumaki T, Tanaka A *J. Appl. Phys.* **97** 10N119 (2005)
6. Yuan H et al. *J. Appl. Phys.* **103** 07F513 (2008)
7. Bethe H A *Phys. Rev.* **66** 163 (1944)
8. García de Abajo F J *Rev. Mod. Phys.* **79** 1267 (2007)
9. Chu Y et al. *Appl. Phys. Lett.* **93** 181108 (2008)
10. Meier M, Wokaun A, Liao P F *J. Opt. Soc. Am. B* **2** 931 (1985)
11. Korringa J *Physica* **13** 392 (1947)
12. Kohn W, Rostoker N *Phys. Rev.* **94** 1111 (1954)
13. Wang X et al. *Phys. Rev. B* **47** 4161 (1993)
14. Bever S J, Allebach J P *Appl. Opt.* **31** 3524 (1992)
15. Gradsteyn I S, Ryzhik I M *Tablitsy Integralov, Summ, Ryadov i Proizvedenii* (Table of Integrals, Series, and Products) (Moscow: Fizmatgiz, 1963) [Translated into English (New York: Academic Press, 1965)]
16. Landau L D, Lifshitz E M *Kvantovaya Mekhanika*: *Nepelyativistskaya Teoriya* (Quantum Mechanics: Non-Relativistic Theory) (Moscow: Nauka, 1989) [Translated into English (Oxford: Pergamon Press, 1977)]
17. Ctistis G et al. *Nano Lett.* **9** 1 (2009)

PACS numbers: 42.25.Gy, **42.55.–f**, **78.67.–n**
DOI: 10.3367/UFNe.0179.200909k.1018

Superresolution and enhancement in metamaterials

A N Lagarkov, A K Sarychev, V N Kissel, G Tartakovsky

1. Introduction

We discuss the optical and microwave properties of artificial materials that can have negative dielectric and magnetic constants simultaneously. Backward electromagnetic waves can propagate in such metamaterials, which leads to a negative refraction. We discuss some unusual properties of metamaterials, in particular, the effect of superresolution. The large losses predicted in such materials in optics can be compensated by using an amplifying laser medium. We also consider the possibility of designing a nanolaser with a size several dozen times less than the wavelength of light. This article is intended as a general introduction to this thriving field.

More than 100 years have passed since Lamb's work appeared [1], where he first noted the possibility of the existence of backward waves, i.e., unusual wave processes with oppositely directed phase and group velocities. The properties of backward electromagnetic waves were also discussed by Schuster [2]. Almost simultaneously, in the article "Growth of a wave-group when the group velocity is negative," Pocklington [3] showed that in a medium that supports backward waves, a point source excites *convergent* waves, and the group velocity of waves is directed from the source. These works did not attract much attention for almost 40 years, until the well-known work of Mandel'shtam [4] was published, in which he predicted a new physical phenomenon, the negative refraction. This phenomenon can exist only in the case where the refracted waves propagate in a medium that supports backward waves. A discussion of article [4] can be found, for example, in recent work [5].

The next important step was made by Sivukhin in Ref. [6], where it was first shown that in a medium with simultaneously negative dielectric (ε) and magnetic (μ) permeabilities, the group and phase velocities of the wave are oppositely directed. Until the appearance of Ref. [6], this sufficiently fine circumstance remained unnoticed, possibly because the wave equation preserves its form in the case of a simultaneous change of the signs of ε and μ.